BUTTERWORTH HEINEMANN

Modeling of waste heat recovery by looped water-in-steel heat pipes

M. Akyurt, N. J. Lamfon, Y. S. H. Najjar, M. H. Habeebullah, and T. Y. Alp
College of Engineering, King Abdulaziz University, Jeddah, Saudi Arabia

Modeling and simulation of a water-in-steel heat pipe heat recovery system is undertaken in this paper. The heat recovery system consists of a looped two-phase thermosyphon that receives heat from the stack of a gas turbine engine and delivers it to the generator of an NH_3-H_2O absorption chiller. Variations in the operating temperature as well as evaporator geometry are investigated, and the consequences on system effectiveness are studied. It is concluded that the model for the water-in-steel looped thermosyphon overcomes drawbacks of the water-in-copper thermosyphon, and that the steel system is simpler in design, lower in cost, and more competent in performance.

Keywords: absorption chiller; gas turbine engine; heat pipe; heat recovery; looped thermosyphon; modeling; stack

Introduction

In many circumstances heat that is otherwise wasted can be effectively and economically recovered and reused. Various types of heat transfer equipment commonly used for recapturing waste heat were discussed in Al-Rabghi et al. (1993). Of these, heat pipes with excellent thermal and design merits emerge as devices that are efficient in transporting heat (Akyurt et al. 1993). A heat recovery system based on a looped heat pipe was proposed by Lamfon et al. (1994a 1994b) to reuse waste heat from a gas turbine engine.

Thermal performance of an ordinary wick-type heat pipe has been studied extensively (Arora and Domkundwar 1987; Asselman and Green 1973; Azad and Geoola 1984; Azad and Gibbs 1987; Azad et al. 1985; Chi 1976; Dunn and Reay 1978; Huang and Tsuei 1985; Shiraishi et al. 1981; and Stulc and Vasiliev, 1985). Huang and Tsuei predicted the performance of the heat pipe by thermal resistance modeling. A modeling and simulation study for the thermal operation of long heat pipes was also effected (Gari and Fathalah, 1988). Thermodynamic analysis of heat pipe operation was investigated by Vasiliev and Konev (1982). An exergy balance was made to obtain an expression for thermodynamic efficiency of heat pipes.

The maximum heat transfer of a two-phase thermosyphon was investigated by Pioro (1983, 1985). Theoretical studies on the steady-state characteristics and stability thresholds on closed two-phase thermosyphons were presented by Dorban (1985). Gross and Hahne (1986) investigated the heat transfer performance of closed thermosyphons over wide ranges of pressure and inclination angles. Heat transfer performance of corrugated tube two-phase thermosyphons was reported by Hirashima et al. (1989).

A simulation study of the closed thermosyphon heat exchanger was made by Kamiya et al. (1991). Experimental tests on an R-113 charged thermosyphon were conducted. Good agreement between the simulation and the experimental results was obtained. Negishi et al. (1991), on the other hand, studied the performance of a two-phase corrugated tube thermosyphon charged with distilled water. The influence of liquid charge ratio and inclination angle on heat transfer performance were studied. It was found that the optimum ratio of liquid charge to evaporator volume was 40%, and the maximum performance was obtained at an inclination angle of 30°.

Fukuda et al. (1991) tested a thermosyphon fitted with a glass portion, with vapor and condensate flows separated. The goals of the test were to avoid condensate flooding and to increase heat transfer. Tests with stainless still double tubes revealed that the limits for the thermosyphon are greatly increased by separation of liquid and vapor streams (Fukuda et al.). Joudy et al. (1991) also reported improved heat transfer performance with an internal wall that separated the liquid and vapor streams.

Experimental as well as theoretical studies on the performance of heat pipe heat exchangers have also been reported. The heat transfer effectiveness of heat pipe heat exchangers was studied by Peretz (1982), who found that the HTE (heat transfer effectiveness) of the heat exchanger depends upon the HTE of a single heat pipe, the number of rows parallel to the flow, and the ratio of heat capacities of the two fluids. The thermal performance of heat pipe heat recovery system was investigated by Azad et al. (1985). A model for the system was developed to predict the temperature distribution in longitudinal rows of the heat exchanger. The mathematical simulation considered the performance of heat exchanger row-by-row, and the overall effectiveness was also calculated (Azad et al.).

The effectiveness of gravity-assisted air-to-air heat exchangers was studied by Wadowski et al. (1991). The study concluded that a minimum temperature difference between the two airstreams is required in order to initiate operation. When full operation power is reached, the effectiveness becomes independent of the temperature difference of the two airstreams.

Address reprint requests to Dr. M. Akyurt, Mechanical Engineering Department, King Abdulaziz University, P.O. Box 9027, Jeddah 21413, Saudi Arabia.

Received 20 January 1994; accepted 13 December 1994

Int. J. Heat and Fluid Flow 16: 263–271, 1995

655 Avenue of the Americas, New York, NY 10010

0142-727X/95/$10.00
SSDI 0142-727X(94)00023-6

Water-to-air gravity-assisted heat pipe heat exchangers were likewise investigated (Azad and Gibbs 1987; Azad and Moztarzadeh 1985). The overall effectiveness of heat exchanger was calculated for a wide range of parameters. The NTU-ε approach was used to analyze a coaxial heat pipe heat exchanger. The design procedure was presented by Azad and Geoola (1984), and models for heat transfer resistances in heat pipes were also given. Optimization of heat pipe heat exchangers has been studied (Peretz and Horbaniuc 1984). The optimization procedure allows the selection of such heat exchanger parameters as equilateral triangular pitch and heat capacities ratios to give maximum heat exchanger effectiveness and/or heat flow per unit weight.

It is well known that water is excellent as a working fluid for heat pipes because of its high latent heat, its availability, and its high resistance to decomposition and degradation. Water has been used particularly successfully in copper heat pipes for low temperature applications. Because its vapor pressure increases rapidly above 100°C, water must be used with casing materials of higher strength when temperatures exceed about 150°C. For water heat pipes working in the range 150 to 300°C, plain carbon steel, preferably with low carbon content, would be considered to be a natural replacement for copper. Problems of incompatibility, however, are reported in the literature (Akyurt 1984 1986; Basiuhs 1976; Chi 1976; Dunn and Reay 1978; Reay 1982, 1983; and Seshan and

Notation

A	reference area, m^2
C	heat capacity, kW/K
COP	coefficient of performance
Cp	specific heat at constant pressure, kJ/kg·K
Cv	specific heat at constant volume, kJ/kg·K
D	diameter, m
g	acceleration of gravity, m/s^2
Gr	Grashof number
h	convection heat transfer coefficient, $W/m^2 \cdot K$
h	enthalpy, kJ/kg
H	enthalpy, kJ/kg
Hc	enthalpy of combustion for the fuel, kJ/kg
k	specific heat ratio
K	thermal conductivity, W/m·K
Lg	length, m
M	mass flow rate, kg/h
Mw	molecular weight, kg/kmol
N	number of pipes
NTU	number of heat transfer unit
Nu	nusselt number
P	pressure, kN/m^2
Pr	Prandtl number
q	surface tension constant
Q	heat rate, W
Q	total heat release rate, kW
r	radius, m
R	specific gas constant, kJ/kg·K
R	thermal resistance, K/W
Re	Reynolds number
SG	specific gravity
T	temperature, K
v	specific volume, m^3/kg
V	velocity, $m^3/kmol$
V	volumetric flow rate, m^3/h
Vm	molecular volume, $m^3/kmol$
x	concentration with mole fraction
X	concentration with mass fraction
Wd	width, m

Greek

δ	thickness, m
Δ	differential (losses)
ε	effectiveness
η	efficiency, %
θ	specific energy constant, kJ/kg
μ	dynamic viscosity, kg/m·s
ρ	density, kg/m^3
σ	surface tension, N/m
υ	kinematic viscosity, m 2/5
ϕ	relative humidity, %
ψ	angle of inclination, rad

Subscripts

a	ambient
act	actual data from manufacturer charts
ae	evaporator of absorber machine
am	ammonia
ass	assumed value for iteration
ax	auxiliaries
br	brass metal
c	condenser (condensation)
c	compressor
ch	extended exhaust chimney
chw	chilled water
co	copper
cp	specific heat at constant pressure
cs	carbon steel
ct	condensate tube
e	evaporator (vaporization)
exh	exhaust
eq	equivalent
f	film (average)
g	generator
h	enthalpy
ins	insulation
l	losses
lm	laminar flow
lq	liquid
m	manufacturer design data
max	maximum
mech	mechanical losses due to lubricating oil
min	minimum
mt	material
p	pipe
r	ratio
re	Reynolds number
s	ammonia–water solution
sa	surface area
sat	saturated
sr	surface area ratio
tia	inlet air of gas turbine engine
v	vapor
vr	vertical
vt	vapor tube
w	wall
wa	water
wr	welding rod

Vijayalakshmi 1986) when water is used with plain carbon steel or alloy steel. The studies confirm that hydrogen is evolved inside iron–water heat pipes, so that the condenser eventually becomes flooded with this noncondensable gas, making the heat pipe inoperative.

Water was selected as the working fluid of the present heat pipe system. Because of the problem of incompatibility with iron, however, copper was selected initially as the container material. Thus, the analysis presented by Lamfon et al. (1994) was developed for a Cu-water heat pipe system. Encouraged by the results of in-house experiments on water-in-steel heat pipes, as well as supportive findings reported in recent literature (Chen et al. 1992 and Tongze and Hou 1989) it was decided to base the heat pipe system to be implemented in the present heat recovery system on mild steel (MS). This decision is sigificant especially from the point view of economic viability. The choice of MS instead of copper as the construction material would be expected to make a very substantial impact on the economic merit of an investment involving heat pipes.

In what follows, we first present a brief review of the overall heat recovery system. The modeling of the water-in-steel thermosyphon loop is taken up next, followed by a discussion of results.

Waste heat recovery system

Because of its simple design and reported outstanding thermal performance, the two-phase thermosyphon loop was selected to extract waste heat from stacks of gas turbine engines and then to deliver this energy to the generator of an aqua–ammonia absorption machine (Figure 1). The refrigeration load for the absorption machine in this case, consists of cooling of the intake air for the compressor of the gas turbine engine. It is expected that cooling of the compressor air will boost output power.

The two ends of the water-charged MS thermosyphon are incorporated in the stack and the generator of the chiller, respectively, and serve as heat transport media between the two. Water is evaporated in the evaporator of the heat pipe loop, the vapor flows through the adiabatic vapor tube and releases its heat of condensation at the generator. The condensate then flows through a separate condensate tube back to the evaporator.

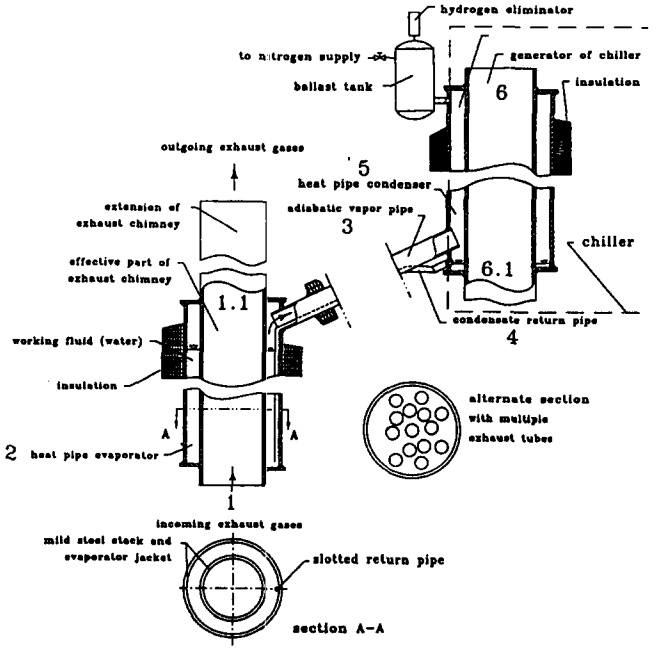

Figure 1 Schematic view of the heat recovery system

Inside the generator, the solution of NH_3-H_2O is heated, and the refrigerant is generated. The nearly pure NH_3 refrigerant that emerges at the top of the generator completes the usual absorption cycle. At the other end of this particular commercial absorption machine, water is circulated through the evaporator of the machine, making it a chiller. Chilled water is then piped to a tube-fin heat exchanger for the purpose of cooling the ambient air. The cold air is then fed to the intake of the compressor of the gas turbine system.

Figure 1 illustrates a fire-tube type of stack fitted with a concentric jacket. Although the sizes and number of tubes needed are to be determined by further investigations, this figure serves to illustrate a general concept for a heat pipe interface at the chimney. Exhaust gases flow through the inner core(s). The insulated annular jacket is the evaporator of the heat pipe. At the top of the jacket is a large diameter (about 150 mm) vapor outlet pipe and a small diameter (about 25 mm) condensate return pipe. The entire system is of welded construction.

Figure 1 depicts also the condenser of the heat pipe as mounted on the generator of the chiller, where the diameter of the generator of the commercial chiller (Chiller's Application Manual 1990) is about 150 mm. The heat pipe condenser, with a diameter of about 200 mm and length of about 700 mm, forms a concentric and insulated jacket around the generator. The vapor tube enters the condenser jacket near the bottom, and the condensate return pipe is placed immediately below it. An opening at the top of the condenser feeds into a 10-l ballast tank for noncondensable gases. The ballast tank is equipped with a hydrogen eliminator.

The heat required at the generator Q_g is calculated from data supplied by the manufacturer of the absorption machine (Chiller's Application Manual 1990). This heat is to be furnished by the condenser of the thermosyphon. Taking care of all thermal resistances between the condenser and the evaporator (i.e., condensation, convection, evaporation, and conduction), we can calculate the mass of the working fluid and the heat Q_{exh} required from exhaust gases at the evaporator of the thermosyphon. Naturally, pressure variation inside the thermosyphon is also modeled. Losses such as generator loss $Q_{g,l}$, condenser losses $Q_{l,c}$, condensate tube losses $Q_{l,ct}$, vapor tube losses $Q_{l,vt}$, evaporator losses $Q_{l,e}$, and chimney wall losses $Q_{l,exh}$ are modeled and considered in the calculations.

Simulation of the looped two-phase thermosyphon

Thermal resistances between chimney and generator are evaluated by using existing relationships or derived correlations that have been introduced elsewhere (Lamfon et al., 1994a). These include the thermophysical properties of substances such as flue gases, water (vapor and liquid), and aqua–ammonia.

The simulation procedure commences at the generator (Figure 2). Thus, the heat Q_g required at the generator is found from data suppied by the manufacturer of the chiller. Analysis for the looped two-phase thermosyphon is undertaken next, starting from the condenser back to the evaporator, including all heat losses to the ambient. In this manner, it is possible to determine the heat that must be supplied to the evaporator. Finally, the heat that must be extracted from exhaust gases is found.

Generator of the absorption system

Heat transferred to generator. The temperature of saturated ammonia $T_{\mathrm{am,sat}}$ can be found once the generator pressure $P_{s,g}$ is known. Temperatures $T_{i,s,g}$ and $T_{o,s,g}$ of saturated solution at inlet and outlet of the generator are functions of $T_{\mathrm{am,sat}}$ and ammonia mass faction at generator inlet $X_{\mathrm{am},i}$ and outlet $X_{\mathrm{am},o}$, respectively. Average temperature $T_{f,s,g}$ of saturated solution in the generator is related to $T_{\mathrm{am,sat}}$ and average mass fraction of ammonia $X_{\mathrm{am},f,g}$. Average mole fraction $x_{\mathrm{am},f,g}$ of ammonia is estimated by using $X_{\mathrm{am},f,g}$, molecular weights of water Mw_{wa} and ammonia Mw_{am}. The densities $\rho_{\mathrm{lq},s,g}$ and $\rho_{v,s,g}$ of liquid and vapor solutions of aqua–ammonia, respectively, are functions of $T_{f,s,g}$, $X_{\mathrm{am},f,g}$, $P_{s,g}$ and solution gas constant $R_{s,g}$. Heat of evaporation $H_{\mathrm{lq},v,s,g}$ and specific heat $\mathrm{Cp}_{\mathrm{lq},s,g}$ of liquid solution are also evaluated.

Dynamic viscosity $\mu_{\mathrm{lq},s,g}$ of generator liquid solution is related to $x_{\mathrm{wa},f,g}$, $\mu_{\mathrm{lq,wa},g}$, $x_{\mathrm{am},f,g}$ and $\mu_{\mathrm{lq,am},g}$. Thermal conductivity $K_{\mathrm{lq},s,g}$ of generator liquid solution is a function of $K_{\mathrm{lq,wa},g}$ and $K_{\mathrm{lq,am},g}$. Also surface tension $\sigma_{s,g}$ of generator solution depends upon $\sigma_{\mathrm{wa},g}$ and $\sigma_{\mathrm{am},g}$. Internal surface area $A_{\mathrm{sa},i,g}$ of generator wall is calculated by the use of inside diameter $D_{i,g}$ and length Lg_g of the generator,

$$A_{\mathrm{sa},i,g} = \pi * D_{i,g} * Lg_g \tag{1}$$

Temperature $T_{w,i,g}$ of inner surface of the generator is estimated by the following relation for boiling phenomena (Rohsenow 1952; Incropera and DeWitt 1990)

$$T_{w,i,g} = T_{f,s,g} + \left(\frac{0.013 * H_{\mathrm{lq},v,s,g} * Pr_{\mathrm{lq},s,g}}{Cp_{\mathrm{lq},s,g}}\right) * \left(\frac{Q_g}{A_{\mathrm{sa},i,g} * \mu_{\mathrm{lq},s,g} * H_{\mathrm{lq},v,s,g}}\right)^{0.33} * \left(\frac{\sigma_{s,g}}{g * (\mu_{\mathrm{lq},s,g} - \mu_{v,s,g})}\right)^{0.33/2} \tag{2}$$

whereas, temperature $T_{w,o,g}$ of outside surface of the generator is estimated based on heat conduction through the generator wall.

$$T_{w,o,g} = T_{w,i,g} + Q_g/\{[2 * \pi * \mathrm{Lg}_g/\mathrm{Ln}(r_{o,g}/r_{i,g})] * K_{\mathrm{mt},g}\} \tag{3}$$

where the shell of the generator is made of mild steel with a thermal conductivity of $K_{\mathrm{mt},g}$.

Heat pipe condenser

Heat loss to surrounding. External temperature $T_{w,o,c}$ of condenser wall is assumed initially and confirmed later. Insulation radii of condenser shell (internal $r_{\mathrm{ins},i,c}$ and external $r_{\mathrm{ins},o,c}$) are computed. Temperature $T_{o,\mathrm{ins},c}$ of the external surface of insulation at condenser side is initially assumed and then found by iteration. Average temperature $T_{f,\mathrm{ins},c}$ of ambient air in the neighborhood of the external surface of insulation at the condenser is calculated. Physical properties of ambient air at the average ambient temperature $T_{f,a}$ are determined as follows:

$$\mathrm{Gr}_{f,\mathrm{ins},c} = [g * \mathrm{Lg_c}\text{^}3 * (T_{o,\mathrm{ins},c} - T_{f,a})]/(v_{f,a}\text{^}2 * T_{f,\mathrm{ins},c}) \tag{4}$$

$$v_{f,a} = \mu_{f,a}/\rho_{f,a} \tag{5}$$

$$\mu_{f,a} = -9.9246 * 10\text{^}{-7} + 8.9129 * 10\text{^}{-8} * T_{f,a} - 9.6364 * 10\text{^}{-11} * T_{f,a}\text{^}2 + 7.3003 * 10\text{^}{-14} * T_{f,a}\text{^}3 - 2.7106 * 10\text{^}{-17} * T_{f,a}\text{^}4 + 3.8332 * 10\text{^}{-21} * T_{f,a}\text{^}5 \tag{6}$$

$$\rho_{f,a} = 1.2935 - 4.5039 * 10\text{^}{-3} * T_{f,a} + 1.2391 * 10\text{^}{-5} * T_{f,a}\text{^}2 - 2.1871 * 10\text{^}{-8} * T_{f,a}\text{^}3 + 2.0797 * 10\text{^}{-11} * T_{f,a}\text{^}4 - 7.9712 * 10\text{^}{-15} * T_{f,a}\text{^}5 \tag{7}$$

$$\mathrm{GrPr}_{f,\mathrm{ins},c} = \mathrm{Gr}_{f,\mathrm{ins},c} * \mathrm{Pr}_{f,\mathrm{ins},c} \tag{8}$$

$$\mathrm{Pr}_{f,\mathrm{ins},c} = \mu_{f,a} * Cp_{f,a}/K_{f,a} \tag{9}$$

$$Cp_{f,a} = 1018.9134 - 0.13783636 * T_{f,a} + 1.9843397 * 10\text{^}{-4} * T_{f,a}\text{^}2 + 4.2399242 * 10\text{^}{-7} * T_{f,a}\text{^}3 - 3.7632489 * 10\text{^}{-10} * T_{f,a}\text{^}4 \tag{10}$$

$$K_{f,a} = -2.0838 * 10\text{^}{-3} + 1.1979 * 10\text{^}{-4} * T_{f,a} - 1.0233 * 10\text{^}{-7} * T_{f,a}\text{^}2 + 7.8979 * 10\text{^}{-11} * T_{f,a}\text{^}3 - 3.1564 * 10\text{^}{-14} * T_{f,a}\text{^}4 + 5.2848 * 10\text{^}{-18} * T_{f,a}\text{^}5 \tag{11}$$

$$h_{f,a,\mathrm{lm}} = \{1.42 * [(T_{o,\mathrm{ins},c} - T_{f,a})/\mathrm{Lg_c}]\text{^}0.25\} \quad \text{for laminar flow} \tag{12}$$

$$h_{f,a,tr} = [0.95 * (T_{o,\mathrm{ins},c} - T_{f,a})\text{^}(1/3)] \quad \text{for turbulent flow} \tag{13}$$

Heat loss $Q_{l,c}$ to ambient from the condenser is determined by using relationships for conduction and convection phenomena.

$$Q_{l,c} = [2 * \pi * \mathrm{Lg_c} * (T_{w,o,c} - T_a)]/\{[\mathrm{Ln}(r_{\mathrm{ins},o,c}/r_{\mathrm{ins},i,c})/K_{\mathrm{mt,ins}}] + [1/(r_{\mathrm{ins},o,c} * h_{f,a,\mathrm{lm}})]\} \tag{14}$$

Temperature $T_{o,\mathrm{ins},c}$ of the external surface of insulation at the condenser is evaluated by the following convection relation and is found by iteration. This and other temperatures mentioned below are computed with a tolerance value of 0.01% or better.

$$T_{o,\mathrm{ins},c} = T_a + \{Q_{l,c}/[h_{f,a,\mathrm{lm}} * (2 * \pi * r_{\mathrm{ins},o,c} * \mathrm{Lg_c})]\} \tag{15}$$

Heat transferred from heat pipe condenser. Temperature $T_{c,v}$ of the condensed water vapor is assumed initially and it is found by iteration. Temperatures of the condensed liquid and of the water vapor are assumed to be identical. Average temperature $T_{c,f}$ of condensed water vapor and internal wall of the condenser is evaluated as follows:

$$T_{c,f} = \{T_{c,v} + \mathrm{T}_{w,i,c}\}/2 \tag{16}$$

Reynolds number $\mathrm{Re}_{c,f}$ of condensed water at average temperature is calculated by the following condensation relation:

$$\mathrm{Re}_{c,f} = (4/3) * \{\{4 * K_{c,\mathrm{lq}} * \mathrm{Lg_c} * \rho_{c,\mathrm{lq}}^{2/3} * [g * \sin(\psi_c)]\}^{1/3} * (T_{c,v} - T_{w,i,c})/(H_{\mathrm{lq},v,re} * \mu_{c,\mathrm{lq}}^{5/3})\}^{3/4} \tag{17}$$

where

$$H_{\mathrm{lq},v,\mathrm{re}} = H_{\mathrm{lq},v,f} + [(3/8) * Cp_{c,\mathrm{lq}} * (T_{c,v} - T_{w,i,c})] \tag{18}$$

In the above equations, $H_{\mathrm{lq},v,f}$ is heat of evaporation of condensate water, and $Cp_{c,\mathrm{lq}}$ is condensate specific heat. The $\mathrm{Re}_{c,f}$ computed above is used for determining the flow retgime. Convection heat transfer coefficients $h_{c,f,\mathrm{lm}}$ for laminar flow, and $h_{c,f,\mathrm{tr}}$ for turbulent flow are estimated at the average

temperature by the following (Incropera and DeWitt, 1990):

$$h_{c,f,\mathrm{lm}} = 0.943 * \{[\rho_{c,\mathrm{lq}} * (\rho_{c,\mathrm{lq}} - \rho_{c,v}) * H_{\mathrm{lq},v,\mathrm{re}} * g * \sin(\psi_c) * K_{c,\mathrm{lq}}^3]/[\mu_{c,\mathrm{lq}} * \mathrm{Lg}_c * (T_{c,v} - T_{w,i,c})]\}^{0.25} \quad (19)$$

$$h_{c,f,\mathrm{tr}} = 0.056 * [K_{c,\mathrm{lq}}^3 * \rho_{c,\mathrm{lq}}^2 * g * \sin(\psi_c)/\mu_{c,\mathrm{lq}}^2]^{1/3} * \mathrm{Re}_{c,f}^{0.2} * \mathrm{Pr}_{c,\mathrm{lq}}^{0.5} \quad (20)$$

Temperature $T_{c,v}$ of condensed water is evaluated by the following relationship for convection.

$$T_{c,v} = T_{w,o,g} + [Q_g/(h_{c,f,\mathrm{lm}} * A_{\mathrm{sa},o,g})] \quad (21)$$

where $h_{c,f}$ is the heat transfer coefficient, found by Equation 19 or 20, and

$$A_{\mathrm{sa},o,g} = \pi * D_{o,g} * \mathrm{Lg}_g \quad (22)$$

Saturated pressure $P_{c,\mathrm{lq}}$ of condensed water is evaluated by using the saturation pressure–saturation temperature relation.

Adiabatic condensate tube

Heat transfer parameters. Temperature $T_{o,\mathrm{ct}}$ of external surface of condensate tube is assumed initially and then checked by iteration. Average temperature $T_{f,\mathrm{ct}}$ of condensate in the tube is the mean of $T_{o,\mathrm{ct}}$ and $T_{c,\mathrm{lq}}$. Average velocity $V_{f,\mathrm{ct}}$ of condensate flow is calculated by the following relationship:

$$V_{f,\mathrm{ct}} = M_{c,\mathrm{lq}}/(\rho_{f,\mathrm{ct}} * A_{i,\mathrm{ct}}) \quad (23)$$

where $A_{i,\mathrm{ct}}$ is internal surface area of condensate tube, and $\rho_{f,\mathrm{ct}}$ is condensate density. Reynolds number $\mathrm{Re}_{f,\mathrm{ct}}$ of condensed water at average temperature of condensate tube is computed by the following:

$$\mathrm{Re}_{f,\mathrm{ct}} = 4 * M_{c,\mathrm{lq}}/(\pi * D_{i,\mathrm{ct}} * \mu_{f,\mathrm{ct}}) \quad (24)$$

and Nusselt numbers $\mathrm{Nu}_{f,\mathrm{ct,lm}}$ and $\mathrm{Nu}_{f,\mathrm{ct,tr}}$, for laminar and turbulent flow, respectively, are evaluated by the relations following (Incropera and DeWitt 1990):

$$\mathrm{Nu}_{f,\mathrm{ct,lm}} = 4.364 \quad (25)$$

$$\mathrm{Nu}_{f,\mathrm{ct},tr} = 0.023 * \mathrm{Re}_{f,\mathrm{ct}}^{0.8} * \mathrm{Pr}_{f,\mathrm{ct}}^{0.4} \quad (26)$$

Average heat transfer coefficients $h_{f,\mathrm{ct,lm}}$ and $h_{f,\mathrm{ct,tr}}$ for condensate flow are based on Nu values computed in the above equations.

Heat loss to surrounding. Heat loss $Q_{l,\mathrm{ct}}$ from condensate tube is evaluated by the following:

$$Q_{l,\mathrm{ct}} = M_{c,\mathrm{lq}} * Cp_{f,\mathrm{ct}} * (T_{c,\mathrm{lq}} - T_{o,\mathrm{ct}}) \quad (27)$$

where $M_{c,\mathrm{lq}}$ is condensate mass flow rate. Temperatures $T_{w,i,\mathrm{ct}}$ and $T_{w,o,\mathrm{ct}}$ of the internal wall of the condensate tube is estimated by the following:

$$T_{w,i,\mathrm{ct}} = T_{f,\mathrm{ct}} - Q_{l,\mathrm{ct}}/(\pi * D_{i,\mathrm{ct}} * \mathrm{Lg}_{ct} * h_{f,\mathrm{ct},tr}) \quad (28)$$

$$T_{w,o,\mathrm{ct}} = T_{w,i,\mathrm{ct}} - [Q_{i,\mathrm{ct}} * Ln(r_{o,\mathrm{ct}}/r_{i,\mathrm{ct}})/(2 * \pi * \mathrm{Lg}_{ct} * K_{\mathrm{mt,ct}})] \quad (29)$$

where

$$K_{\mathrm{mt,ct}} = 36.532 + 0.049157 * T_{w,i,\mathrm{ct}} - 1.0404 * 10\text{^}-4 * T_{w,i,\mathrm{ct}}\text{^}2 + 4.8307 * 10\text{^}-8 * T_{w,i,\mathrm{ct}}\text{^}3 \quad (29)$$

Temperature $T_{o,\mathrm{ins,ct}}$ of external surface of insulation of condensate tube is assumed initially and is then checked by iteration. Physical properties of ambient air at average ambient temperature are calculated using the relationships given elsewhere (Lamfon et al. 1994a). Temperature $T_{o,\mathrm{ins,ct}}$ of external surface of insulation on condensate tube is evaluated by the following convection relationship:

$$T_{o,\mathrm{ins,ct}} = T_a + [Q_{l,\mathrm{ct}}/(A_{\mathrm{sa},o,\mathrm{ins,ct}} * h_{f,a})] \quad (30)$$

$$A_{\mathrm{sa},o,\mathrm{ins,ct}} = 2 * \pi * r_{\mathrm{ins},o,\mathrm{ct}} * \mathrm{Lg}_{ct} \quad (31)$$

Average temperature $T_{f,\mathrm{ct}}$ of condensed water is evaluated by the following conduction/convection relationship:

$$T_{f,\mathrm{ct}} = T_{i,\mathrm{vt}} + \{[Q_{l,\mathrm{ct}}/(2 * \pi * \mathrm{Lg}_{\mathrm{ct}})] * [1/(r_{i,\mathrm{ct}} * h_{f,\mathrm{ct},tr})] + (Ln(r_{o,\mathrm{ct}}/r_{i,\mathrm{ct}})/K_{\mathrm{mt,ct}}) + [1/(r_{o,\mathrm{ct}} * h_{w,o,\mathrm{ct},tr})]\} \quad (32)$$

where $K_{\mathrm{mt,ct}}$ is thermal conductivity of condensate tube evaluated at average temperature.

Variation of pressure. Velocity $V_{i,\mathrm{ct}}$ of condensate at inlet of condensate tube, and velocity $V_{o,\mathrm{ct}}$ of condensate at outlet of condensate tube are evaluated. The outlet pressure $P_{o,\mathrm{ct}}$ of condensate in the condensate tube is determined by the following Bernoulli equation:

$$P_{o,\mathrm{ct}} = \rho_{o,ct} * \{(P_{i,\mathrm{ct}}/\rho_{i,\mathrm{ct}}) + [(V_{i,\mathrm{ct}}^2 - V_{o,\mathrm{ct}}^2)/2] + [g * (\mathrm{Lg}_{\mathrm{vr,ct}} + \mathrm{Lg}_{\mathrm{eq,ct}} * \tan\{\psi_{\mathrm{ct}}\})]\} \quad (33)$$

$$P_{i,\mathrm{ct}} = P_{c,\mathrm{lq}} \quad (34)$$

Saturated temperature $T_{o,\mathrm{ct,sat}}$ at outlet pressure of condensate is evaluated from the vapor–pressure relation.

Adiabatic vapor tube

Heat transfer parameters. Inlet temperature $T_{i,\mathrm{vt}}$ of vapor in vapor tube is assumed initially and is then determined by iteration. Heat transfer parameters of saturated steam inside the vapor tube are calculated by relationships similar to those of the condensate tube.

Heat loss to surrounding. Heat loss from water vapor through the vapor tube and the insulation to ambient is evaluated by a model similar to that of the condensate tube. These equations, along with the required iterations, lead to the computation of heat loss $Q_{l,\mathrm{vt}}$ from the vapor tube to ambient.

Variation of pressure. Inlet pressure at vapor tube and equivalent saturated vapor temperature are determined by relations similar to those of condensed water:

$$P_{i,\mathrm{vt}} = \rho_{i,\mathrm{vt}} * \{P_{o,\mathrm{vt}}/\rho_{o,\mathrm{vt}}\} + [(V_{o,\mathrm{vt}}^2 - V_{i,\mathrm{vt}}^2)/2] + \{g * [\mathrm{Lg}_{\mathrm{eq,vt}} * \tan(\psi_{\mathrm{vt}})]\}\} \quad (35)$$

$$P_{o,\mathrm{vt}} = P_{c,\mathrm{lq}} \quad (36)$$

Inlet pressure of saturated steam is recalculated by using the gas relation:

$$P_{i,\mathrm{vt}} = R_{\mathrm{wa,vt}} * \rho_{i,\mathrm{vt}} * T_{i,\mathrm{vt}} \quad (37)$$

$$R_{\mathrm{wa,vt}} = P_{o,\mathrm{vt}}/(\rho_{o,\mathrm{vt}} * T_{o,\mathrm{vt}}) \quad (38)$$

Heat pipe evaporator

Heat transferred to heat pipe evaporator. Evaporator working temperatures for liquid water $T_{e,\mathrm{lq}}$ and water vapor $T_{e,v}$ have the saturated temperature $T_{o,\mathrm{ct,sat}}$ at outlet condensate pressure

$$T_{e,v} = T_{o,\mathrm{ct,sat}} \quad (39)$$

Velocity $V_{e,v}$ of water vapor inside the heat pipe evaporator is estimated by the following:

$$V_e = M_e/(\rho_{v,e} * A_{i,e}) \tag{40}$$

The required heat Q_e to be transferred to the evaporator is related to the heat delivered by the condenser, the heat loss from the condensate tube and vapor tubes, and the appropriate geometry of the condenser and evaporator of the heat pipe system.

$$Q_e = Q_{l,w,vt} + Q_c \tag{41}$$

The net heat Q_e that is transferred from the exhaust chimney to the evaporator is recalculated using Equation 42. This equation is based on the requirement that the heat delivered to the evaporator must equal the heat required to increase the condensate temperature from $T_{o,ct}$ to $T_{lq,e}$, in addition to supplying the heat of vaporization and superheating of steam to $T_{i,v}$.

$$Q_e = M_e * [Cp_{i,lq,e} * (T_{i,e,sat} - T_{o,ct}) + H_{lq,v,e} + Cp_{o,v,e} * (T_{i,vt} - T_{i,e,sat})] \tag{42}$$

Temperature $T_{w,i,e}$ of internal surface of evaporator tube is estimated by the boiling relation. Convection heat transfer coefficient h_e is then calculated by using $T_{w,i,e}$, and equations similar to Equations 1 and 2.

Heat loss to surroundings. External temperature $T_{w,o,e}$ of the wall of the evaporator tube is computed by the conduction relationship through the evaporator shell of thermal conductivity $K_{mt,e}$. The heat loss $Q_{i,e,p}$ to ambient from the evaporator tube and heat transfer parameters are determined by relationships similar to those for the condenser shell. Additionally, temperature $T_{o,ins,e}$ of the external surface of the insulation on the evaporator is evaluated by iteration. The external wall temperature $T_{w,o,exh}$ of the exhaust pipe(s) is estimated by the following:

$$T_{w,o,exh} = T_e + \{\{(0.013 * H_{lq,v,e} * Pr_{lq,e}/Cp_{lq,e}) * [Q_{exh,w}/(A_{sa,o,exh} * \mu_{lq,e} * H_{lq,,e})]\text{^}(0.33) * (\sigma_{lq,e}/\{g * \{\rho_{lq,e} - \rho_{v,e}\}]\}\text{^}(0.33/2)\} \tag{43}$$

where

$$Pr_{lq,e} = \mu_e * Cp_e/K_e \tag{44}$$

$$\mu_{lq,e} = 8.565 * 10\text{^}-6 * \exp(32.483 - 0.20129 * T_{c,f} + 4.8867 * 10\text{^}-4 * T_{c,f}\text{^}2 - 3.9533 * 10\text{^}-7 * T_{c,f}\text{^}3 - 1.9283 * 10\text{^}-10 * T_{c,f}\text{^}4 + 3.2256 * 10\text{^}-13 * T_{c,f}\text{^}5) \tag{45}$$

$$K_{lq,e} = -0.47719 + 0.0060505 * T_e - 8.7168 * 10\text{^}-6 * T_e\text{^}2 + 2.1886 * 10\text{^}-9 * T_e\text{^}3 \tag{46}$$

$$\sigma_{lq,e} = 0.080832 + 1.315 * 10\text{^}-4 * T_e - 6.629 * 10\text{^}-7 * T_e\text{^}2 + 4.0604 * 10\text{^}-10 * T_e\text{^}3 \tag{47}$$

$$\rho_{lq,e} = -6318.1 + 74.291 * T_e - 0.27622 * T_e\text{^}2 + 4.5236 * 10\text{^}-4 * T_e\text{^}3 - 2.936 * 10\text{^}-7 * T_e\text{^}4 + 2.7842 * 10\text{^}-11 * T_e\text{^}5 \tag{48}$$

$$A_{sa,o,exh} = \pi * D_{o,exh} * Lg_{exh} \tag{49}$$

Exhaust pipe of gas turbine engine

Heat loss to surrounding at evaporation section. Internal temperature $T_{w,i,exh}$ of the mild steel exhaust wall is computed by the following conduction relationship:

$$T_{w,i,exh} = T_{w,o,exh} + \{(Q_{exh,w}/N_{exh,p}) * Ln(r_{o,exh}/r_{i,exh})/\{2 * \pi * Lg_{exh} * K_{mt,exh}\}\} \tag{50}$$

where $N_{exh,p}$ is the number of exhaust pipes and

$$K_{mt,exh} = 36.532 + 0.049157 * T_{w,o,exh} - 1.0404 * 10\text{^}-4 * T_{w,o,exh}\text{^}2 + 4.8307 * 10\text{^}-8 * T_{w,o,exh}\text{^}3 \tag{51}$$

Average exhaust temperature $T_{f,exh}$ of exhaust gases is assumed initially and is determined by iteration. Outlet temperature $T_{o,exh}$ of exhaust gases is evaluated. Exhaust mass flow M_{exh} required for each exhaust pipe is calculated by using the following:

$$M_{exh} = Q_{exh,w}/[Cp_{exh} * (T_{i,exh} - T_{o,exh})] \tag{52}$$

The average exhaust flow velocity V_{exh} at the exhaust pipe is determined by the following:

$$V_{exh} = 4(M_{exh}/N_{exh,p})/(\pi\rho_{exh} * A_{eq,exh} * D_{i,exh}\text{^}2) \tag{53}$$

where $\rho_{f,exh}$ is evaluated by Equation 7.

Reynolds number $Re_{f,exh}$ of exhaust gases at average temperature $T_{f,exh}$ is calculated by the following:

$$Re_{exh} = 4(M_{exh}/N_{exh,p})/(\pi * D_{i,exh} * A_{eq,exh} * \mu_{f,exh}) \tag{54}$$

where $\mu_{f,exh}$ is evaluated by Equation 6. The calculated value of the Reynolds number is used for identifying the exhaust flow regime. Nusselt number $Nu_{f,exh}$ of the exhaust flow and the convection heat transfer coefficient $h_{f,exh}$ are evaluated using equations similar to those for condensed water. Average exhaust temperature $T_{f,exh}$ is found by iteration.

$$T_{f,exh} = T_{w,i,exh} + [(Q_{exh,w}/N_{exh,w})/(h_{f,exh} * A_{sa,i,exh})] \tag{55}$$

where $A_{sa,i,exh}$ is expressed by a relation in the form of Equation 22.

Results and discussion

The model developed during the current study allows the investigation of a waste heat recovery system for the extraction of waste energy from exhaust stacks and its delivery to the generator of an aqua–ammonia absorption chiller. The system, shown schematically in Figure 1, consists of the exhaust pipe or pipes, the evaporator, vapor tube, condensate tube and condenser of the thermosyphon, and the generator of the absorption chiller. There is sufficient flexibility built into the model to incorporate various design geometries for the stack and all elements of the looped two-phase thermosyphon. The model also permits the simulation of operational conditions and stack geometries so as to enable detailed studies of the heat recovery system to be undertaken.

This model was employed to simulate the performance of the heat recovery system under various design conditions. It must be pointed out that the design of the condenser was essentially prescribed by the layout of the commercial chiller and its generator. Additionally, the design geometries of the vapor tube and the condensate tube were resolved by an earlier model presented elsewhere (Lamfon et al. 1994). During the current study, particular emphasis was placed, therefore, on the

Table 1 Input data for the model

Generator	Evaporator
Heat required, 29.3 kW Diameter, 0.22 m Length, 0.73 m	Diameter, 0.75 m for single tube Length, 2.2 m
Condenser	Vapor tube
Diameter, 0.27 m Length, 0.73 m	Diameter, 0.15 m Length, 2.0 m
Condensate tube	Exhaust chimney
Diameter, 0.027 m Length, 3.5 m	Diameter, 0.69 m for single pipe Useful length, 2.2 m Inlet temperature, 525 K

geometries of the evaporator and of the chimney. In addition, the effect of operating temperatures on system variables was investigated.

Figure 3 shows the variation of temperatures within the heat recovery system for the case when a single exhaust pipe is utilized. The x-axis in Figure 3 is the location on the heat pipe system with the same notations as given in Figure 1, and the y-axis is the temperature in K. It must be pointed out that the temperatures plotted are *averages*. Thus, the temperature at location 5 in Figure 1 (the condenser of the heat pipe) is the average of the inlet and outlet temperatures of the condenser.

With reference to Figure 3, the following may be observed. The exhaust gas temperature drops around 2 K across the exhaust pipe between points 1 and 1.1. In addition, there is a very sharp drop in temperature, around 115 K, between the gas inside the exhaust pipe and the evaporator of the heat pipe, point 2. The heat pipe is then observed to remain essentially isothermal, as would be expected, until the condenser of the heat pipe, point 5, is reached. A temperature drop of around 30 K at the generator of the chiller provides sufficient potential for heat transfer there. Note that the condensate return pipe is likewise essentially isothermal with the rest of the thermosyphon loop.

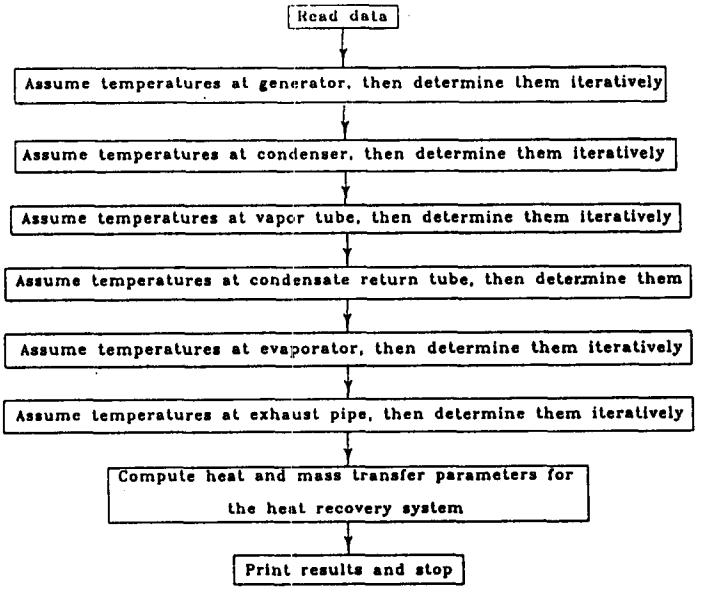

Figure 2 Flowchart of the computation scheme

This graph clearly demonstrates the manner in which the heat pipe acts as a temperature transformer. It receives heat at a relatively high temperature, in the present case 525 K, and conveys it isothermally, and then delivers it at a considerably lower temperature, around 390 K, at the wall of the absorption generator, and this is over a considerable distance.

Next, the number of exhaust pipes passing through the evaporator was varied, keeping the total cross-sectional areas of the exhaust stream constant. The resulting evaporator in the present case resembles a fire-tube boiler. Using data for seamless pipes (schedule 40), a number of runs were made for an exhaust inlet temperature of 525 K. Figure 4 summarizes some of the findings. The points indicated by a solid circle are for pipes of 2-m length; the rest of the symbols refer to pipes of 2.2-m length.

It can be observed from Figure 4 that the temperature of exhaust gases entering the evaporator experience a ΔT drop of about 2° at exit when a single exhaust pipe is used ($N = 1$). The ΔT between inlet and exit rises sharply when the number of pipes is increased. The curve of ΔT rises with steep slopes at first, when the number of pipes is less than 75, and then tapers off as the number of pipes is increased beyond 100 pipes. Because the heat requirement at the generator is fixed, and the heat required from the exhaust pipe is sought, temperatures for points 2–6.1 of Figure 1 do not vary during the present analysis.

The velocity of exhaust gases is reduced from its initial value of 56 m/s for the case of a single exhaust pipe to about 4 m/s for 175 pipes. The mass flow rate of the exhaust stream that is required to supply the needed heat is reduced from its initial value of 13.5 kg/s to about 2 kg/s for $N = 20$. The mass flow-rate curve is observed to remain essentially flat as the number of pipes is increased. This stagnancy in mass flow rate is especially noticeable when the number of pipes exceeds about 50.

The observation from Figure 4 that the required mass flow rate remains essentially constant for $N > 50$ leads to an interesting conclusion. Because the rate of energy recovered from the exhaust stream depends upon the mass flow rate as well as ΔT, a decision on pipe size; i.e., number of pipes to be used, may be based on ΔT. This is especially true because ΔT continues to rise when $N > 50$.

It would also be of interest to study the effect of exhaust temperature on flow parameters. Figure 5 displays the variation of ΔT, mass flow rate, and gas velocity as the inlet temperature of exhaust gases is raised from 525 to 825 K for $N = 114$ ($2\frac{1}{2}$ in.

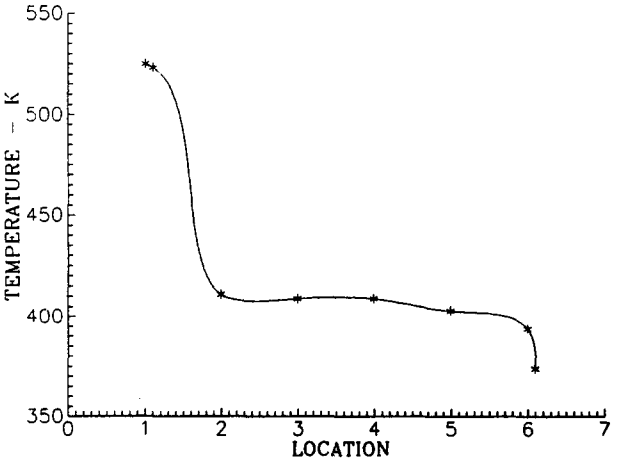

Figure 3 Variation of temperature along the heat recovery system (single pipe)

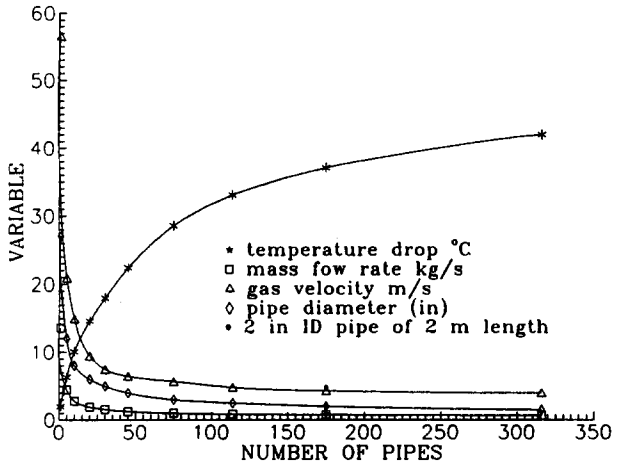

Figure 4 Variation of exhaust flow parameters with number of pipes at 525 K

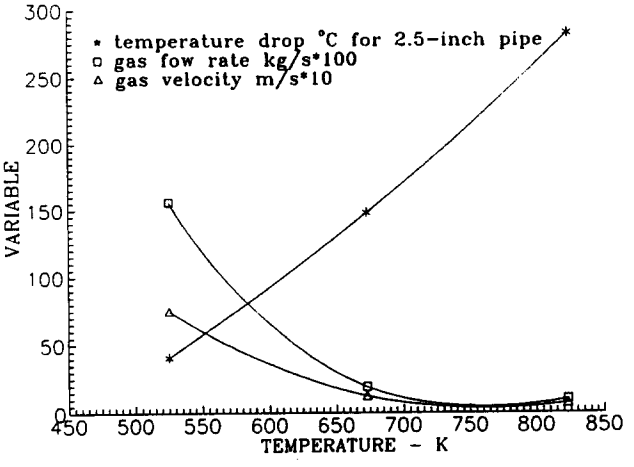

Figure 5 Variation of flow variables with exhaust temperature for 114 pipes

i.d. pipe). The ΔT is observed to rise with vigor from about 32° to about 285°. The mass flow rate and the gas velocity decrease rapidly at first, and then gradually.

Figure 5 seems to demonstrate that it is clearly advantageous to keep exhaust temperatures above 650 K. This becomes evident when it is noticed that ΔT keeps rising, while mass flow rate decreases at a slower pace in this region.

Conclusions

The model developed for the water-in-steel type of looped thermosyphon system clearly overcomes drawbacks of the water-in-copper thermosyphon. The new system is simpler in design, lower in cost, and more competent in performance. Thus, resistance to heat transfer is reduced by replacing a maze of copper tubes, brazings, and steel linings by steel linings alone. This is true both at the generator of the chiller and the evaporator of the heat pipe. The cost advantages of mild steel as compared to copper are evident.

A very significant advantage of the steel thermosyphon is the improved performance it offers. This is because the steel thermosyphon readily lends itself to the adoption of a fire-tube type of heat exchanger design at the evaporator, which is in contrast to the restrictions imposed by the copper thermosyphon. Thus, for the copper thermosyphon, the highest ΔT drop in the temperature of exhaust gases between inlet and outlet of the chimney was predicted to be about 7°C when the inlet temperature was 673 K (Lamfon et al. 1994). The corresponding ΔT predicted for a steel thermosyphon is 115°C (Figure 5). Assuming that the threshold temperature for heat recovery is 473 K, efficiency η of heat recovery may be expressed as follows:

$$\eta = \frac{\Delta T}{673 - 473}$$

whence the efficiencies would be 3.5% and 57.5% for the copper and steel systems, respectively.

Acknowledgment

This work was sponsored by King Abdulaziz City for Science and Technology, Riyadh, Saudi Arabia through grant no AR-12-39.

References

Akyurt, M. 1984. Development of heat pipes for solar water heaters. *Solar Energy*, **32**, 625–631

Akyurt, M. 1986. AWSWAH—the heat pipe solar water heater. *J. Eng. Appl. Sci.*, **3**, 23–38

Akyurt, M., Beirutty, M., Al-Rabghi, O. M., Najjar, Y. S. H. and Alp, T. 1993. Heat pipes for heat recovery. *Trans. Mech. Eng.*, **ME18**, 221–234

Al-Rabghi, O. M., Akyurt, M., Najjar, Y. S. H. and Alp, T. 1993. Heat exchangers for waste heat recovery. *Energy and Environ., Alert* **4**, 284–306

Arora, S. C. and Domkundwar, S. 1987. *A Course in Heat and Mass Transfer*, J. C. Kapoor, New Delhi

Asselman, G. A. and Green, D. B. 1973. Heat pipes. *Philips Tech. Rev.*, **33**, 104–113

Azad, E. and Geoola, F. 1984. Design procedure for gravity-assisted heat pipe heat exchanger. *J. Heat Recov. Sys.*, **4**, 101–111

Azad, E. and Gibbs, B. M. 1987. Analysis of air-to-water heat pipe heat exchanger. *J. Heat Recov. Sys.*, **7**, 351–358

Azad, E., Mohammadieh, F. and Moztarzadeh, F. 1985. Thermal performance of heat pipe recovery system. *J. Heat Recov. Sys.*, **5**, 561–570

Azad, E. and Moztarzadeh, F. 1985. Design of air-to-water co-axial heat pipe heat exchanger. *J. Heat Recov. Sys.*, **5**, 217–224

Basiulis, A. 1976. Compatibility and reliability of heat pipe materials. *Int. Heat Pipe Conf. 2nd, Eur. Space Agency*, **1**, 357–372

Chen, E. J., Chen, I. Y. and Wan, K. M. 1992. Steel-water heat pipe employing hydrogen oxidizing means. *Proc. 8th Intern. Heat Pipe Conf.*, Beijing Sept. 14–18, Internal Academic Publishing, Beijing, 499–503

Chi, S. W. 1976. *Heat pipe theory and practice*, Hemisphere, Washington, DC, 242 pp

Chillers Application Manual, Dometic Corp., Evansville, IN

Dorban, F. 1985. Steady-state characteristics and stability thresholds of a closed two-phase thermosyphon. *Int. J. Heat Transfer*, **28**, 949–957

Dunn, P. D. and Reay, D. A. 1978. *Heat Pipes*, 2nd ed., Pergamon, New York

Fukuda, K., Hasegawa, S. and Kondoh, T. 1991. Thermal characteristics of double-tube two-phase thermosyphon. *Nippon Kikai Gakkai Ronbunsku B Hen*, **57**, 687–692

Gari, H. A. and Fathalah, K. A. 1988. Modeling and simulation of a passive condensate heat pipe pumping system for solar energy applications. *Heat Recov. Sys. & CHP*, **8**, 559–569

Gross, U. and Hahne, E. 1986. Heat transfer in closed thermosyphon over a wide range of pressures and inclinations. *Ger. Chem. Eng.*, **9**, 292–299

Hirashima, M., Nishikawa, Y. and Taguchi, M. 1989. Heat transfer performance of corrugated-tube thermosyphons. *Nippon Kikai Gakkai Ronbunshu B Hen*, **55**, 3778–3782

Huang, B. S. and Tsuei, J. T. 1985. Method of analysis for heat pipe heat exchangers. *Int. J. Heat Mass Transfer*, **28**, 553–562

Incropera, F. and DeWitt, D. 1990. *Fundamentals of Heat and Mass Transfer*, 3rd ed., Wiley, New York

Joudy, K. A., Husain, T. A. and Abdulmajeed, P. M. 1991. Improved heat transport of heat pipes with an internal wall separating liquid and vapor streams. *Energy Converg. Mgmt.*, **31**, 141–148

Kamiya, Y., Cheng, K. C. and Tokumu, M. 1991. Simulation study and operating characteristics of an air-to-water heat exchanger using a closed-loop two-phased thermosyphon system. *Proc. 3rd ASME/JSME Thermal Engineering Joint Conf., Part 5*, Reno, NV

Lamfon, N., Akyurt, M., Al-Rabghi, O. M. and Najjar, Y. S. H. 1994a. Thermophysical relationships for waste heat recovery using looped heat pipes. *Int. J. Energy Res.*, **18**. 633–642

Lamfon, N. J., Akyurt, M., Najjar, Y. S. H. and Al-Rabghi, O. M. 1994. Performance of a waste heat recovery system using looped heat pipes. *Power and Energy Sys.*, (accepted)

Negishi, K., Kanji, K., Matsuoka, T. and Hirashima, M. 1991. Heat transfer performance of a corrugated-tube thermosyphon, Part 1, Evaporator performance. *Heat Transfer—Japan. Research*, **20**, 144–157

Peretz, R. 1982. Heat transfer effectiveness of heat pipes. *Heat Recov. Sys.*, **2**, 165–172

Peretz, R. and Horbaniuc, B. 1984. Optimal heat pipe heat exchanger design. *J. Heat Recov. Sys.*, **4**, 9–24

Pioro, I. L. 1983. Maximum heat transfer capability two-phase thermosyphons. *Heat Transfer Sov. Res.*, **15**, 24–31

Pioro, I. L. 1985. Correlation of experimental data on the maximum heat and mass transfer in two-phase thermosyphons. *Heat Transfer Sov. Res.*, **17**, 75–83

Reay, D. A. 1982. The Perkins tube—A noteworthy contribution to heat exchanger technology. *J. Heat Recov. Sys.*, **2**, 173–187

Reay, D. A. 1983. The European Community energy R & D program—Report on a recent contractors meeting on heat exchangers and heat recovery. *J. Heat Recov. Sys.*, **3**, 245–271

Rohsenow, W. M. 1952. A method of correlation heat transfer data for surface boiling liquids. *Trans. ASME*, **74**, 969

Seshan, S. and Vijayalakshmi, D. 1986. Heat pipes—Concepts, materials, and applications. *Energy Convers. Mgmt.*, **26**, 1–9

Shiraishi, M., Kikuchi, K. and Yamanishi, T. 1981. Investigation of heat transfer characteristics of a two-phased closed thermosyphon. *J. Heat Recov. Sys.*, **1**, 287–297

Stulc, P. and Vasiliev, L. L. 1985. Heat pipe heat exchangers in heat recovery system. *J. Heat Recov. Sys.*, **5**, 415–418

Tongze, M. and Zengqi, H. 1989. Heat pipe research and development in China. *Heat Recov. Sys. & CHP*, **9**, 499–512

Vasiliev, L. L. and Konev, S. V. 1982. *Thermodynamic Analysis of Heat Pipe Operation, Advances in Heat Pipe Technology*, 1st ed., Pergamon, Tarrytown, New York, 313–325

Wadowski, T., Akbarzadeh, A. and Johnson, P. 1991. Characteristics of a gravity-assisted heat pipe based heat exchanger. *J. Heat Recov. Sys. & CHP*, **11**, 69–77